N73 15030

NASA TECHNICAL MEMORANDUM

NASA TM X- 68167

NASA TM X- 68167

FLAP NOISE MEASUREMENTS FOR STOL CONFIGURATIONS USING EXTERNAL UPPER SURFACE BLOWING

by Robert G. Dorsch, Meyer Reshotko
and William A. Olsen
Lewis Research Center
Cleveland, Ohio

TECHNICAL PAPER proposed for presentation at
Eighth Propulsion Joint Specialists Conference sponsored
by the American Institute of Aeronautics and Astronautics
and the Society of Automotive Engineers
New Orleans, Louisiana, November 29 - December 1, 1972

E-7227

FLAP NOISE MEASUREMENTS FOR STOL CONFIGURATIONS USING EXTERNAL UPPER SURFACE BLOWING

by Robert G. Dorsch, Meyer Reshotko, and William A. Olsen

Lewis Research Center
National Aeronautics and Space Administration
Cleveland, Ohio

Abstract

Screening tests of upper surface blowing EBF configurations were conducted. Noise and turning effectiveness data were obtained with small-scale, engine-over-the-wing models. One large model was tested to determine scale effects. Nozzle types included circular, slot, D-shaped, and multilobed. Tests were made with and without flow attachment devices. For STOL applications the particular multilobed mixer and the D-shaped nozzles tested were found to offer little or no noise advantage over the round convergent nozzle. High aspect ratio slot nozzles provided the quietest configurations. In general, upper surface blowing was quieter than lower surface blowing for equivalent EBF models.

Introduction

Short takeoff and landing (STOL) aircraft will be using airports located close to large population centers. The noise generated by these airplanes must be at levels acceptable to the nearby community. This is a difficult engineering task because the lift augmentation devices generate and redirect noise. For example, the use of externally blown flaps for jet powered lift augmentation results in considerable flap interaction noise below the airplane.[1-4]

A possible solution to the STOL powered lift noise problem is to locate the engines above the wing. Externally blown flap (EBF) STOL airplane configurations utilizing upper surface blowing for lift augmentation (fig. 1) may have an inherent advantage from a noise standpoint.[5-9]

Locating the engine above the wing takes advantage of "built in" shielding of the high frequency components of the exhaust noise by the wing surfaces during flyover.

Good flow attachment to the flaps is required for powered lift. Various schemes can be used to achieve attachment of the engine exhaust flow. Some of the schemes are illustrated in Fig. 2. The first configuration (shown at the top of fig. 2) is for an engine having a slot-shaped exhaust nozzle. The exhaust nozzle is located close to the wing surface to facilitate flow attachment. The second configuration uses a conventional circular nozzle with a flow deflector to turn the flow towards the flaps. The flow deflector is retracted for cruise or CTOL flight. The flow deflector can also be designed to convert to a thrust reverser after touchdown. The third configuration has a slot nozzle assembly that can be canted downwards towards the flap system to obtain flow attachment. The nozzle is rotated back to its cruise position as the flaps are retracted. The lower sketch of Fig. 2 shows a slot nozzle in combination with sideplates or wing fences to facilitate flow attachment.

Noise sources associated with upper surface flap blowing are illustrated in Fig. 3. The most prominent noise is the low-frequency trailing edge noise. Some of the attachment methods, (such as the flow deflector) introduce considerable impingement noise in the process of directing the flow to the wing and flap surfaces. However, with upper surface blowing the wing reflects much of this high frequency noise away from the region below the airplane.

From a propulsion and aerodynamic efficiency standpoint each of the various methods of achieving attached flow and of minimizing the flap noise has certain drawbacks. Test data on the flap noise characteristics of a variety of upper surface blowing EBF configurations are needed so that the propulsion systems engineer can make the necessary tradeoffs between aerodynamic and propulsion efficiency and noise during the preliminary design stage of a commercial STOL aircraft.

A series of configuration screening tests of a variety of upper surface blowing schemes were therefore conducted at the NASA Lewis Research

Center. Noise and static turning efficiency tests were made with small wing section models blown by convergent exhaust nozzles having a nominal equivalent diameter of 2 in.. Tests were made with circular, slot, D-shaped, and multilobed nozzles located at a variety of exhaust nozzle positions above the wing. Tests were made with and without flow deflectors and wing fences. In addition to the small model tests, a large-scale (13-in. diameter nozzle) noise test of one configuration (circular nozzle with deflector) was run to check scaling laws and for direct comparison with the engine-under-the-wing EBF data of Ref. 2.

The resulting jet and flap noise directivity and spectral data are summarized in this paper. The noise and static turning effectiveness data for the various external upper surface blowing configurations tested are compared and evaluated. The effects of exhaust deflectors, wing shielding, flap-slot covering, nozzle shape, and nozzle canting, are discussed. The effect of a dominant internal noise in the nozzle exhaust is also considered. The results are compared with equivalent EBF configurations utilizing lower surface blowing and the relative advantages from a noise standpoint are discussed.

Apparatus and Procedure

Noise Test Facilities

Small-scale rig. - A typical setup for conducting noise tests on small-scale, engine-over-the-wing models is shown in Fig. 4. The engine exhaust was simulated by an air jet from a convergent nozzle having a nominal diameter of 2 in.. The nozzle was supplied by dried pressurized air at a nominal temperature of 520° R brought to the test site by a 24-in. underground line. The nozzle air supply system consisted of (proceeding downstream) a flow measuring orifice, a flow control valve, two perforated plates, a four-chamber baffled muffler, a 15-ft long, 4-in. diameter inlet pipe and, finally, the nozzle. The muffler was employed to remove internally generated noise (valve, etc.). Background noise at the test site had no effect on the data above 200 Hz.

Sound data were taken by microphones placed on a 10-ft radius centered at the nozzle exit. The microphone plane and jet centerline were located 5 ft above the ground. The engine-over-the-wing EBF model was designed so that it could be rotated about the nozzle centerline axis (fig. 5). Flyover noise was measured with the wing-flap system oriented vertically and making a 90° angle with the horizontal microphone plane (fig. 5(a)). Sideline noise measurements were taken with the nozzle and wing-flap system making a 26.5° angle with the microphone plane (fig. 5(b)).

Large-scale rig. - The large model noise tests were conducted with the facility described in Ref. 2. The wing section was mounted vertically with the nozzle centerline located $12\frac{3}{4}$ ft above grade. Like the small rig the exhaust nozzle was supplied by dried pressurized air at ambient temperature. The microphones were placed in a 50 ft circle in a plane parallel to the ground and passing through the nozzle centerline (flyover noise). Sideline noise measurements were obtained with microphones suspended above the model with a boom.

Models

Small-scale models. - Four typical test model configurations are shown in Fig. 6. Figure 6(a) shows the model configuration with circular exhaust nozzle plus a flow deflector. The configuration with the 5-1 slot nozzle is shown in Fig. 6(b) and with the D-shaped nozzle in 6(c). The mixer nozzle (lobed orifice plate) configuration is shown in Fig. 6(d).

All tests were conducted with the wing at 5° angle of attack with respect to the nozzle centerline. Details of the wing and double-slotted flap system are given in Refs. 1 and 4. The flaps could be set at the 30°-60°, 10°-20°, and 0° (retracted) positions. The flap angles were measured with respect to the wing reference chord line. The wing section chord length was 13 in. and the span was 24 in..

The nozzle throat shapes and dimensions of the four different convergent nozzles employed are given in Fig. 7. The nozzle throat shapes shown are: circular, "D"-shaped, 5:1 aspect ratio slot, and 10:1 aspect ratio slot. In addition, an 8-lobe mixer nozzle was simulated (ref. 10) by an 8-lobe orifice plate which is also shown in Fig. 7.

Tests were made with and without flow deflectors and wing fences. In addition, the nozzles were canted downward toward the flaps for some runs.

In order to evaluate the noise effect of the jet passing over the slot leading edges, the model was tested with slots open, partially covered, and fully covered (fig. 8). In Fig. 8(a) the second slot is covered chordwise with 4-in.-wide tape centered under the jet, while in Fig. 8(b) the first slot is covered in a similar manner, and in Fig. 8(c) both slots are thus covered. In Fig. 8(d) the wing and slots are fully covered spanwise as well.

Large model. - The large-scale model was geometrically identical to the small circular nozzle with deflector configuration (fig. 6(a)) but was 6.5 times as large. The large model had a wing chord length of 7 ft and a 13-in.-diameter circular nozzle. The wing section was mounted vertically and had a span of 9 ft. The wing was at a 5° angle of attack with respect to the nozzle centerline and the flap slots were covered.

Lift and Thrust Measurements

Zero-forward-velocity (static) lift and thrust data were obtained for each small-scale nozzle and wing-flap configuration that was tested for noise characteristics. The lift and thrust data were obtained on a separate facility. The force measuring system was isolated from the nozzle air supply system by sending the pressurized air through twin supply lines into a plenum through flexible couplings. The plenum, nozzle, and wing-flap system were free to move in a horizontal plane and in the axial direction. The plenum and model weight was supported by an overhead-cable suspension system. Forward-thrust was measured by a load cell on the nozzle axis upstream of the plenum. Lift was measured by load cell in the same horizontal plane as the axis but perpendicular to it. A 5 to 1 slot nozzle configuration is shown in Fig. 9 mounted in the rig. The traversing probe shown in the figure was used for velocity surveys in the trailing edge region of the wing.

Test Procedure

For each small-scale model configuration tested, noise and lift and thrust measurements were made for a series of nominal nozzle pressure ratios at a nominal stagnation temperature of 520^{o} R. A series of noise tests were also run (at the same nominal pressure ratios and stagnation temperature) with the large model.

The exhaust velocities for each nominal pressure ratio setting were calculated from measured values of nozzle pressure ratio and stagnation temperature. These velocities were used in the analysis of the acoustic data.

In some runs an orifice plate was used to create a dominant internal noise in the nozzle exhaust flow. This internal noise exceeded all the aerodynamic noises of the experiment. The orifice plate contained four external 0.4 in. diameter holes and was located 6.7 ft upstream of the nozzle exhaust plane.

The sound data were analyzed by a 1/3 octave band spectrum analyzer. The analyzer determined sound pressure level spectra referenced to 0.0002 microbar. Overall sound pressure levels were computed from the SPL data.

The noise data presented herein were not corrected for ground effects. It was found that they had only a small effect on the overall sound pressure levels. Further the ground effect cancellations and reinforcements occuring in the spectra generally do not cause serious problems when comparing the noise data for the various configurations.

Results and Discussion

Flow Attachment

It is important in STOL EBF engine-over-the-wing (EOW) configurations that the exhaust flow have good attachment to the flap system. The lift and thrust data provide a measure of the degree of flow attachment to the upper surface of the flaps and a measure of the turning efficiency of the various test configurations under static conditions. The measured values of static lift and thrust for some of the better attachment cases are summarized in Fig. 10.

Static turning efficiencies are shown in Fig. 10(a) for the flaps in the 10^{o}-20^{o} takeoff position. The flap slots were completely covered in all cases shown. The ordinate is the measured lift force divided by the nozzle alone thrust. The abscissa is the forward thrust divided by the nozzle alone thrust. The turning angle is measured with respect to the engine axis. Data are shown for four configurations, which are listed in the same order as shown in Fig. 2. The configurations have a 10 to 1 aspect ratio slot nozzle, a circular nozzle with deflector, a canted 5 to 1 slot nozzle, and a 5 to 1 slot nozzle with sideplates. Good attachment was achieved, and the flow turned approximately 30^{o} in all cases. Static turning efficiencies between 0.77 and 0.93 are indicated. These values are comparable to those obtained with various engine under the wing EBF models.

The data for the 30^{o}-60^{o} flap position are given in Fig. 10(b). This setting would be typical for landing. At this larger turning angle the circular nozzle with deflector and the canted 5 to 1 slot nozzle configurations still have very good flow attachment. The turning angle is about 60^{o}, and the efficiencies are nearly the same as for the lower flap-angle case. However, the data for the 10 to 1 slot nozzle with no attachment device and for the 5 to 1 slot nozzle with sideplates indicate that the flow attachment was not as good at this flap setting. The lift factors for these two cases, however, are roughly comparable with the circular nozzle plus deflector case.

It was found that at the static conditions of these tests having the flap slots open caused only a small effect on flow attachment. However, as will be shown later, open slots had a large effect on noise.

Circular Nozzle

The mixed flow circular convergent nozzle is of practical interest in EOW applications because it has relatively low internal flow losses and requires the least engine exhaust nozzle redesign. However, for STOL applications (in contrast to CTOL) the use of either a flow deflector or a canted nozzle is required in order to obtain the needed flow attachment to the flaps.

Circular nozzle with deflector. - Typical 1/3-octave sound pressure level (SPL) spectra (referenced to 0.0002 microbar) for the circular nozzle with deflector configuration are shown in Fig. 11 for nozzle exhaust velocities of 750 and 585 ft/sec. Both flap slots were completely covered and the flaps were in the 10°-20° takeoff positon for Fig. 11(a) and in the 30°-60° landing position for Fig. 11(b). The three curves shown in Fig. 11(a) and (b) are the spectra for the 2-in. diameter nozzle alone, the nozzle with the deflector, and the nozzle with deflector above the wing. Figure 11 shows that when the deflector is added to the nozzle, the noise level increases over the nozzle-alone case at all frequencies and particularly at the higher frequencies. When the wing is added, a significant change in the spectrum occurs. The high frequencies are effectively shielded by the wing surface; however, considerable low-frequency trailing-edge noise is generated as the flow exhausts at the trailing edge. The high-frequency part of the spectrum will make an important contribution to the perceived noise level when these model data are scaled up to a full-sized aircraft. The low-frequency noise is important not only because of its contribution to the perceived noise level, but because of the effect of vibration on aircraft and community structures and on cabin interior noise.

The overall sound pressure level (OASPL) radiation pattern at 10 ft radius is shown in polar form in Fig. 12 for a nozzle exhaust velocity of 585 ft/sec. The flap position was 30°-60° and the slots were covered. For comparison, data for the equivalent engine under the wing EBF configuration [4] are also shown. The flap slots were open with lower surface blowing. The engine above the wing radiation pattern is less directional and is about 7 dB quieter at 90° than that for the engine below the wing model.

The OASPL at 80° from the inlet is shown in Fig. 13 as a function of nozzle exhaust velocity for the same engine over the wing test configuration. The nozzle-alone data follow the well-known 8th power law. The nozzle plus deflector and nozzle with deflector plus wing follow a 6th power law and have very similar magnitudes in spite of considerably different spectral characteristics (fig. 11).

The data shown in Figs. 11, 12 and 13 were taken in the flyover plane. Data were also taken with the microphones at the 26.5° sideline position (fig. 5). Flyover and sideline noise spectra at 10 ft are compared in Fig. 14 for the same test conditions as Fig. 11(a). Figure 14 shows that the SPL is less at all frequencies when the microphone is at the 26.5° sideline position. This results in an OASPL decrease of about 3 dB.

The effect of having the flap slots open instead of covered is shown in Fig. 15. Data taken with open and with closed slots (fully covered, fig. 8(d)), are compared at takeoff conditions in Fig. 15(a). Similar data with the flaps in the landing position are shown in Fig. 15(b). Figure 15(c) also contains data with both slots partially covered. Figure 15 shows that the noise level is very sensitive to whether or not the slots are covered. The flap noise is considerably quieter below the wing with the slots fully covered. Also, Fig. 15(c) shows that with both slots partially covered by a 4-in. wide strip of tape (fig. 8(c)), the noise level was about midway in between the open and fully covered cases. The slots were also partially covered one at a time (figs. 8(a) and (b)). Covering only the first slot had a bigger effect than covering only the second slot.

Because of the large effect on flap noise, data will only be presented for engine over-the-wing configurations having fully covered slots from this point on.

The effect of flap position on the 1/3-octave SPL spectra is shown in Fig. 16. OASPL values for the two flap positions are also listed. Although the OASPL does show a small increase with flap deflection angle, Fig. 16 shows that the effect of flap angle on the spectrum is quite small.

Canted circular nozzle. - By canting the exhaust nozzle downward toward the flaps (fig. 2), flow attachment can be achieved with the 10°-20° flap setting without the use of a deflector. One-third-octave SPL data for a canted circular nozzle configuration at 120° from the engine inlet are shown as solid square symbols in Fig. 17. The exhaust velocity was 750 ft/sec, and the flaps were at the 10°-20° position. The spectrum for the deflector arrangement at the same conditions is also plotted on this figure as open circular symbols. The spectra for each of these attached-flow cases are about the same. As a further comparison, the nozzle was blown over the slotless wing with no attachment. This spectrum is shown by the diamond symbols. The two attached-flow cases have additional low-frequency trailing-edge noise. For the conditions noted in this figure, the spectra for all the wing cases come together at high frequency, regardless of the degree of attachment. Of interest also is that because of shielding, the high frequency noise below the model wing is less than that for the nozzle alone.

"D" Nozzle

The "D" shaped nozzle is essentially a circular nozzle flattened on the bottom so that it can be placed close to the wing upper surface. At low aspect ratios, it approaches a circular nozzle in flow attachment characteristics. For example, a 2 to 1 aspect ration "D" nozzle (without flow deflector) was found to provide very little flow attachment (and turning). However, because the nozzle exhaust flow is immediately adjacent to the wing, the noise tests indicated that there was an increase in noise compared to the circular nozzle (without deflector) because of scrubbing action.

The use of a flow deflector with the 2 to 1 aspect ratio "D" nozzle provides attachment and turning efficiencies comparable to those obtained with a circular nozzle with deflector. Noise spectra for this configuration with the flap set at 10^{o}-20^{o} angle are shown in Fig. 18. The data were taken at 100^{o} from the inlet and are shown for three nozzle exhaust velocities. Data for the circular nozzle with deflector configuration are also shown for comparison. The spectra for the "D" and circular nozzles with deflectors are very similar at all three exhaust velocities. Thus from the standpoint of noise, the 2 to 1 aspect ratio "D" nozzle does not appear to offer any advantage for powered lift applications over the circular nozzle. The choice between the two will therefore depend on aerodynamic, structural, and operational considerations.

Mixer Nozzle

The mixer nozzle is another possible candidate for EOW configurations because of its high exhaust velocity decay rate which should reduce the low frequency flap noise. In addition, much of the high frequency content of the mixer nozzle noise should be effectively reflected upward and away from ground observers by the wing and flap system.

Sound pressure level data are shown for the 8-lobe mixer nozzle with deflector configuration in Fig. 19. Figure 19(a) contains 1/3-octave spectra at 100° from the inlet for two exhaust velocities. The mixer nozzle and deflector configuration data indicate that the spectra have a 3 dB per octave roll-off above 1 kHz. Circular nozzle with deflector data are also shown for comparison. These data were Strouhal scaled to the mixer nozzle size (2.4-in. equivalent diameter) to facilitate comparison. The mixer nozzle configuration is quieter at low frequencies as expected. However, at high frequency, it was somewhat louder.

The approximately constant 3 dB per octave roll-off at high frequency allows one to use the sound pressure level directivity at a given frequency. Such a plot is useful in estimating the noise radiation pattern for a large model. The SPL directivities for the 10 kHz one-third octave band are plotted for both configurations in Fig. 19(b). The 10 kHz directivity patterns are quite similar. The only exception is the sharp rise in the circular nozzle data at 80° from the inlet. This highly directional noise was broadband and high frequency. This high frequency noise was found to be sensitive to both nozzle and deflector position. Care should therefore be exercised to avoid or minimize these peaks when selecting the nozzle and deflector location.

The data of Fig. 19 indicate that like the "D" nozzle, the 8-lobe mixer nozzle probably has no noise advantage over the circular nozzle for powered lift applications.

Slot Nozzle

The slot nozzle is normally placed immediately adjacent to (or a short distance above) the wing upper surface in order to facilitate flow attachment. At low aspect ratios, it is necessary to employ attachment devices or to cant the nozzle in order to get good flow attachment to the flaps.

Noise spectra for the configurations with the 5 to 1 slot nozzle with various attachment devices are shown in Fig. 20. The spectra are at 120^o from the inlet for the 10^o-20^o flap position and an exhaust velocity of 750 ft/sec. The jet noise for the slot nozzle alone is given by the solid curve. With no device the flow has poor attachment and the spectrum is shown by the circular data points. There is only a small increase in low-frequency noise. At high frequencies the wing shields some of the nozzle exhaust noise. Canting the nozzle toward the flaps or using sideplates resulted in flow attachment. With flow attachment, there is again a large increase in low-frequency noise.

A spectrum for the 5 to 1 slot nozzle with deflector configuration is shown in Fig. 21 for the 30^o-60^o flap position and an exhaust velocity of 585 ft/sec. These data are compared with a spectrum for the corresponding sideplate configuration. The comparison shows that the deflector configuration is 2 to 3 dB louder at high frequencies. Further, the 5 to 1 slot nozzle with deflector configuration was found to be a few dB louder than the circular nozzle with deflector configuration (other test conditions being equal). Figures 20 and 21 show that the device used to obtain flow attachment has only secondary effects on the flap noise.

The spectra for the 10 to 1 slot nozzle configurations are shown for the same test conditions as Fig. 20 in Fig. 22. At this flap setting, good flow attachment can be achieved without a device. As with the 5 to 1 nozzle, the use of a device had only secondary effects on the noise spectrum. The 10 to 1 slot nozzle configuration is, however, quieter than the 5 to 1 configuration over most of the spectrum (allowing for the somewhat smaller throat area of the 10 to 1 nozzle).

The OASPL radiation patterns for the 5 to 1 and 10 to 1 slot nozzle configurations are compared in polar form in Fig. 23. The 10 to 1 data have been scaled to the same throat area as the 5 to 1 slot nozzle to facilitate comparison. Also shown for reference is a radiation pattern for the engine below the wing EBF configuration (2 in. circular nozzle) of Ref. 4 for the same test conditions. Both slot nozzle configurations are quieter than the engine below the wing model. Further, the 10 to 1 slot nozzle configuration is considerably quieter at all angles than the 5 to 1 configuration.

The 10 to 1 slot nozzle configuration is quieter than the 5 to 1 configuration primarily because the ratio of the length of the wing-flap shielding region, L, to the slot height, h, is larger for the 10 to 1 slot nozzle. This ratio is an important parameter because at large values of L/h the wing shielding (or upward reflection) is very effective because the wave length of much of the noise generated is small compared to L.

The effect of L/h on the noise level below the wing is shown more clearly in Fig. 24. The 5 to 1 and the 10 to 1 slot nozzle configurations have L/h values of 17 and 28 respectively. Also shown are data for the 10 to 1 slot nozzle configuration with an extended flap length giving an L/h of 58.[1] All three spectra have significant low-frequency trailing-edge noise. Increasing L/h results in lower noise levels at 80° from the inlet because of improved shielding. The quietest configuration was the 10 to 1 slot with a 58 to 1 flap-length-to-slot-height ratio. This arrangement is typical of the conventional jet flap where air is supplied from a fan or compressor stage through internal wing ducts. Some consideration has been given to engine over the wing configurations with very high aspect ratio slot nozzles placed say at the 25 percent wing chord station providing high L/h values. The data of Fig. 24 indicate that these configurations would have very good noise shielding characteristics. They would, however, have some of the ducting problems of internally blown systems and might require cruise blowing to be attractive. The 5 to 1 slot nozzle can readily be employed with external upper surface blowing. The 10 to 1 configuration can also be employed for external upper surface blowing configurations by using a fishtail-shaped nozzle or by using two engines in the same pod ("Siamese" installation). If the two-engine "Siamese" installation is used, the engines would have only one-half the thrust of the single engine in order to obtain a good L/h.

Comparison of Good Attachment Cases

Flap noise data for three good attachment cases are summarized in Fig. 25 for take-off conditions. The spectral data are for the circular nozzle with deflector, the 5 to 1 canted slot nozzle, and the 10 to 1 slot nozzle configurations. The 10 to 1 slot nozzle data were scaled to the same nozzle throat area as the 5 to 1 slot nozzle configuration for companion purposes. The spectra have generally similar shapes and levels with the 10 to 1 slot nozzle configuration being the quietest. The data points for the circular nozzle with deflector fall in the middle and are surprisingly close to the 10 to 1 slot nozzle results probably because the effective L/h due to spreading of the jet is better than what one would estimate from nozzle dimensions.

Evaluation of Scale Effects

Scale effects on noise were evaluated from the results of the large-scale engine over-the-wing tests of the circular nozzle with deflector configuration (fig. 26). Typical noise spectra at 50 ft and 90° from the inlet are shown for the large scale model with the flaps in the 30°-60° position in Fig. 27. The nozzle exhaust velocity was 680 ft/sec. Data for the nozzle alone and the nozzle plus wing are given in Fig. 27(a). With the flow deflector removed the flow does not attach so that the main effect below the wing is that of shielding of the jet noise. Figure 27(a) shows that there is good jet noise shielding at all frequencies above 400 Hz. Thus, the engine-over-the-wing location appears to have promise for CTOL applications as well as for powered lift operations. Figure 27(b) gives data with the flow deflector in place. The data are for the nozzle alone, nozzle and deflector, and nozzle plus deflector and wing. As noted with the small-scale model, there is a large increase in noise when the deflector is added to the nozzle. However, again, the wing shields much of this noise from the ground observer at all frequencies above 400 Hz. Also, as noted with the small model there is a large increase in low-frequency noise. Thus, the large model results are very similar to those obtained with the small model when one allows for the shift of the spectrum to lower frequencies. Large model data were also obtained with smaller flap-deflection angles more typical of the takeoff setting. Analysis of data with flaps in the 10^{o}-20^{o} position indicates that the magnitude of the shielding effect is comparable with the 30^{o}-60^{o} results.

In general, the small model data were found to give a reasonably good prediction of the large model results when Strouhal-type scaling[(2)] was used. The agreement was best with the flaps in the 10^{o}-20^{o} position.

Forward Speed Effect

The effects of airplane airspeed on the noise spectra for the small-scale circular nozzle with deflector EOW configuration were determined by free-jet forward-speed-simulation tests (described in ref. 9). Generally, the forward speed effect test showed a small increase in noise (1 to 2 dB below the wing) at frequencies between 600 and 2500 Hz and a decrease in noise (1 to 4 dB) at frequencies above 8000 Hz. The net effect of forward speed on the noise below the wing (80^{o}-100^{o}) was small.

Comparison with Engine-Under-the-Wing

The large model engine over-the-wing EBF noise spectra can be compared with engine-under-the-wing EBF noise spectra using the same 7-ft chord wing and 13-in.-diameter round convergent nozzle.[(2)] In Fig. 28 the upper surface blowing data for the circular nozzle with deflector over the wing configuration are compared with noise data at the same test conditions for the EBF with lower surface blowing. Because of the shielding effect of the wing, upper surface blowing is about 8 dB quieter than lower surface blowing over most of the spectrum. Another difference is that the upper surface blowing spectrum peaks at lower frequency. This effect is somewhat obscured in the data of Fig. 28 by the strong ground effect cancellation occurring at 100 Hz. This low frequency noise could cause more serious vibration problems with upper surface blowing.

The effects of shielding and reflection by the wing flap system can be seen more clearly in Fig. 29. The perceived noise level radiation patterns at 500 ft for the two systems are compared in polar form. The engine over-the-wing system is clearly quieter below the airplane and noisier above. At 90^{o} (or directly below the wing) the flap noise is about 8 PNdB quieter with upper surface blowing.

The perceived noise level data at 500 ft for the two large-scale EBF models are compared in Fig. 30 as a function of nozzle exhaust velocity. The flaps were at the 30^{o}-60^{o} position in both tests, and the flow turning angles and turning efficiencies were comparable. The data are from the microphone angles giving a maximum PNL for flyover in each case. The two curves are nearly parallel, showing the same strong dependence of the noise level on exhaust velocity. Because of shielding, the upper surface blowing data at this flap setting are about 9 PNdB quieter over the velocity range shown. At smaller flap angle settings this difference may be somewhat less.

It should be emphasized that with either engine location the use of powered lift results in the generation of noise as the flow is turned by the flap system. This effect is illustrated in Fig. 31. The shaded region represents (from a simplistic viewpoint) the flow turning noise. Lower surface blowing spectra are shown in Fig. 31(a) at 90^{o} from the inlet for the flaps retracted configuration and with the flaps at the 30^{o}-60^{o} position. Upper surface blowing spectra for the same conditions are shown in Fig. 31(b) for the case of retracted deflector and flaps (unattached flow) and for the 30^{o}-60^{o} flap setting with attached flow. The additional noise due to flow turning is roughly equivalent in the two cases. However, the engine-over-the-wing noise levels are about 8 to 10 dB lower for both attached and unattached flow. Again the effect of shielding is very evident.

Sideline Effects

The data of most of the figures in this paper are representative of flyover noise as they represent noise levels below the wing. Small-scale-model sideline sound pressure level data were given for the circular nozzle with deflector configuration in Fig. 14. Noise data were also obtained with the large model at the wing-tip sideline station (directly above the vertically mounted wing section model) and at the 26.5° sideline station (fig. 5). The perceived noise level at 500 ft from the large-scale model (with a 10°-20° flap setting) for these stations is plotted along with that for the 100° flyover station as a function of nozzle exhaust velocity in Fig. 32. The 500 ft PNL at wing-tip sideline is nearly the same as for the 100° station below the wing over the velocity range shown. However, at the 26.5° sideline station it is 2 to 3 PNdB quieter. Thus the sideline noise for an engine-over-the-wing airplane of this configuration will not exceed the flyover noise level and will generally be smaller.

Shielding of Internal Noise

In addition to the shielding of aerodynamic noise, the upper-surface blowing arrangements should also provide shielding of internal engine noise coming out of the exhaust nozzle; such as the noise from the compressor, fan, and turbine. In other words, with the engine above the wing, the wing and flaps will also shield the community below from some of the internal noise that passes through the exhaust nozzle. The results presented in Fig. 33 show the amount of internal noise reduction, or shielding, in the sideline and flyover planes. The data are for the small model wing section using the 2-in. nozzle with deflector above a slotless wing with a 30°-60° flap position. For this data, internal machinery noise was simulated by placing an orifice upstream of the exhaust nozzle. Noise reductions of 4 to 10 dB were observed. This result is probably conservative. It suggests that less exhaust duct treatment would be required to reduce the perceived internal engine noise below a STOL aircraft with the engine located over the wing than when the engine is below the wing.

Concluding Remarks

The results of this screening study indicate that upper surface blowing is quieter below the wing than lower surface blowing for equivalent EBF configurations. The noise advantage results primarily from the shielding (and redirection) effect of the wing and flaps rather than from a reduction in flap noise generation. That is powered lift is obtained at the expense of a considerable amount of flap noise with both EBF systems. Further, the data indicate that with upper surface blowing the particular method or device used to obtain flow attachment had only secondary effects on the flap noise.

The sensitivity of the noise level to nozzle exhaust velocity is similar to that found for lower surface blowing. Both systems will require some form of flap noise suppression or the use of engines with very low exhaust velocities. Methods of suppressing blown flap noise (including noise generated by flow deflectors) are currently being explored by both Government and aerospace industry research and development groups. Upper surface blowing offers the advantage that less flap noise and turbomachinery suppression are required other factors being equal.

References

1. Dorsch, R. G., Krejsa, E. A., and Olsen, W. A., "Blown Flap Noise Research," Paper 71-745, June 1971, AIAA, New York, N.Y.

2. Dorsch, R. G., Kreim, W. J., and Olsen, W. A., "Externally-Blown-Flap Noise," Paper 72-129, Jan. 1972, AIAA, New York, N.Y.

3. Goodykoontz, J. H., Dorsch, R. G., and Groesbeck, D. E., "Mixer Nozzle-Externally Blown Flap Noise Tests," TM X-68021, 1972, NASA, Cleveland, Ohio.

4. Olsen, W. A., Dorsch, R. G., and Miles, J. H., "Noise Produced by a Small Scale, Externally Blown Flap," TN D-6636, 1972, NASA, Cleveland, Ohio.

5. Dorsch, R. G., Lasagna, P. L., Maglieri, D. J., and Olsen, W. A., "Flap Noise," Aircraft Engine Noise Reduction, SP-311, 1972, NASA, Washington, D.C., pp. 259-290.

6. Reshotko, M., Olsen, W. A., and Dorsch, R. G., "Preliminary Noise Tests of the Engine-Over-The-Wing Concept, I. 30° - 60° Flap Position," TM X-68032, 1972, NASA, Cleveland, Ohio.

7. Reshotko, M., Olsen, W. A., and Dorsch, R. G., "Preliminary Noise Tests of the Engine-Over-The-Wing Concept, II. 10° - 20° Flap Position," TM X-68104, 1972, NASA, Cleveland, Ohio.

8. Dorsch, R. G., and Reshotko, M., "EBF Noise Tests with Engine Under and Over the Wing Configuration," STOL Technology, SP-320, 1972, NASA, Washington, D.C.

9. von Glahn, U., Reshotko, M., and Dorsch, R. G., "Acoustic Results Obtained with Upper-Surface-Blowing Lift-Augmentation Systems," TM X-68159, 1972, NASA, Cleveland, Ohio.

10. Goodykoontz, J. H., Olsen, W. A., and Dorsch, R. G., "Small-Scale Tests of the Mixer Nozzle Concept for Reducing Blown-Flap Noise," TM X-2638, 1972, NASA, Cleveland, Ohio.

E-7227

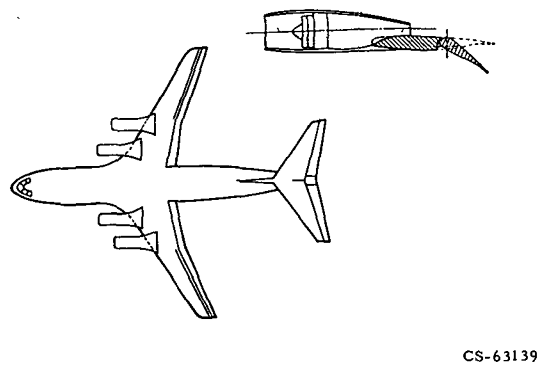

Figure 1. - Externally-blown-flap STOL airplane with upper surface blowing.

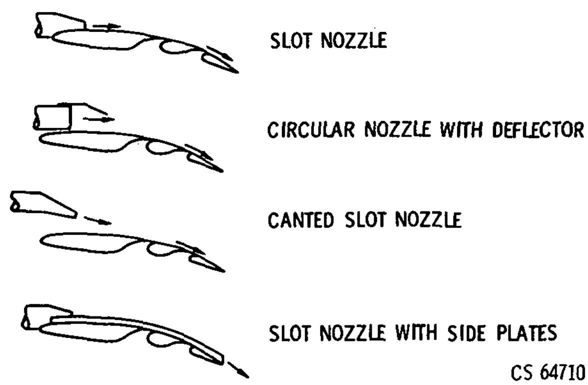

Figure 2. - Some engine-over-the-wing EBF configurations.

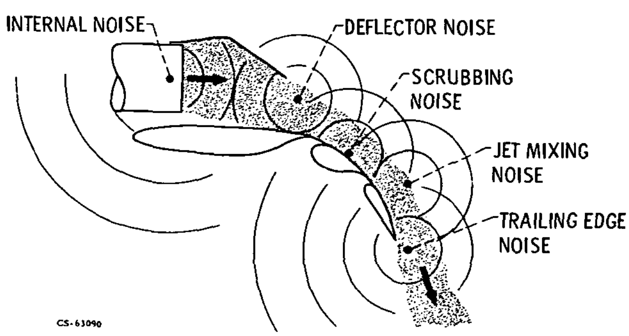

Figure 3. - Noise sources for upper surface flap blowing with deflector configuration.

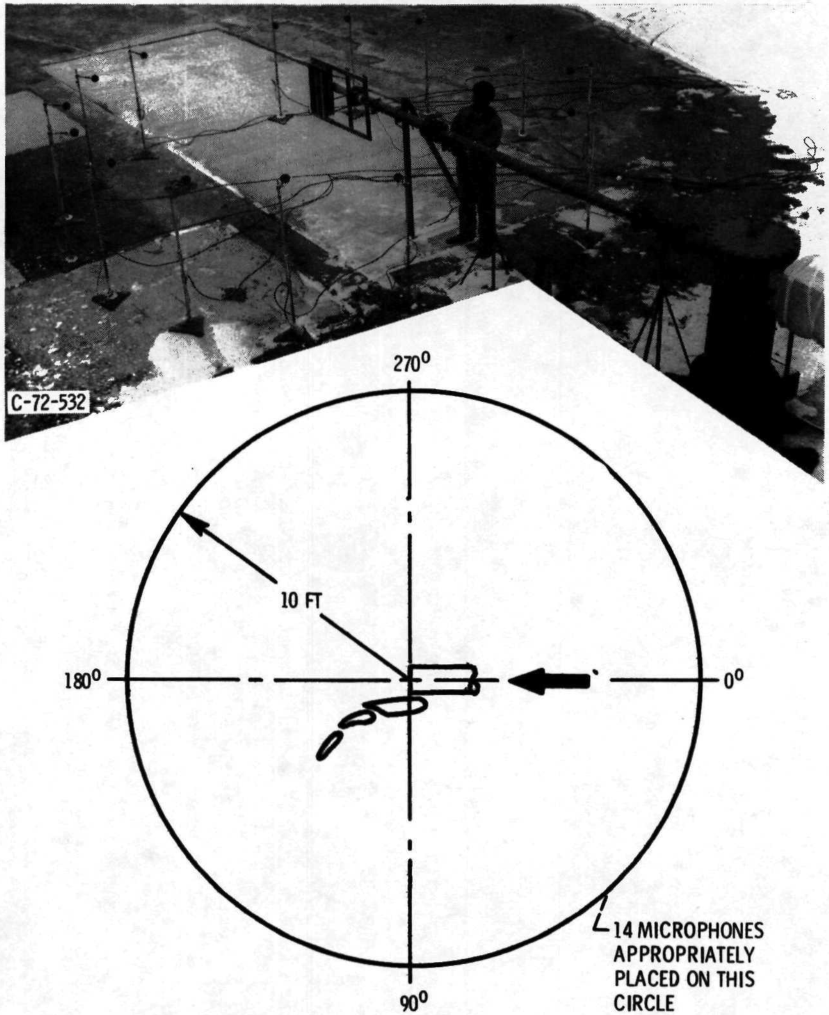

Figure 4. - A typical setup for performing noise tests on the engine-over-the-wing model.

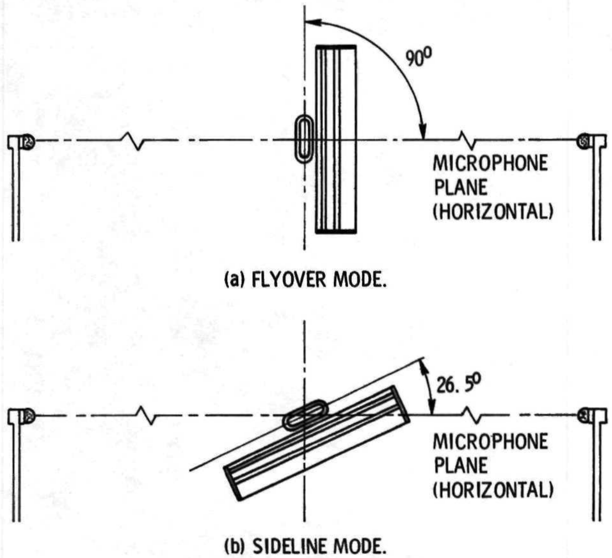

Figure 5. - Typical test configurations of the engine-over-the-wing model in both flyover and sideline modes.

E-7227

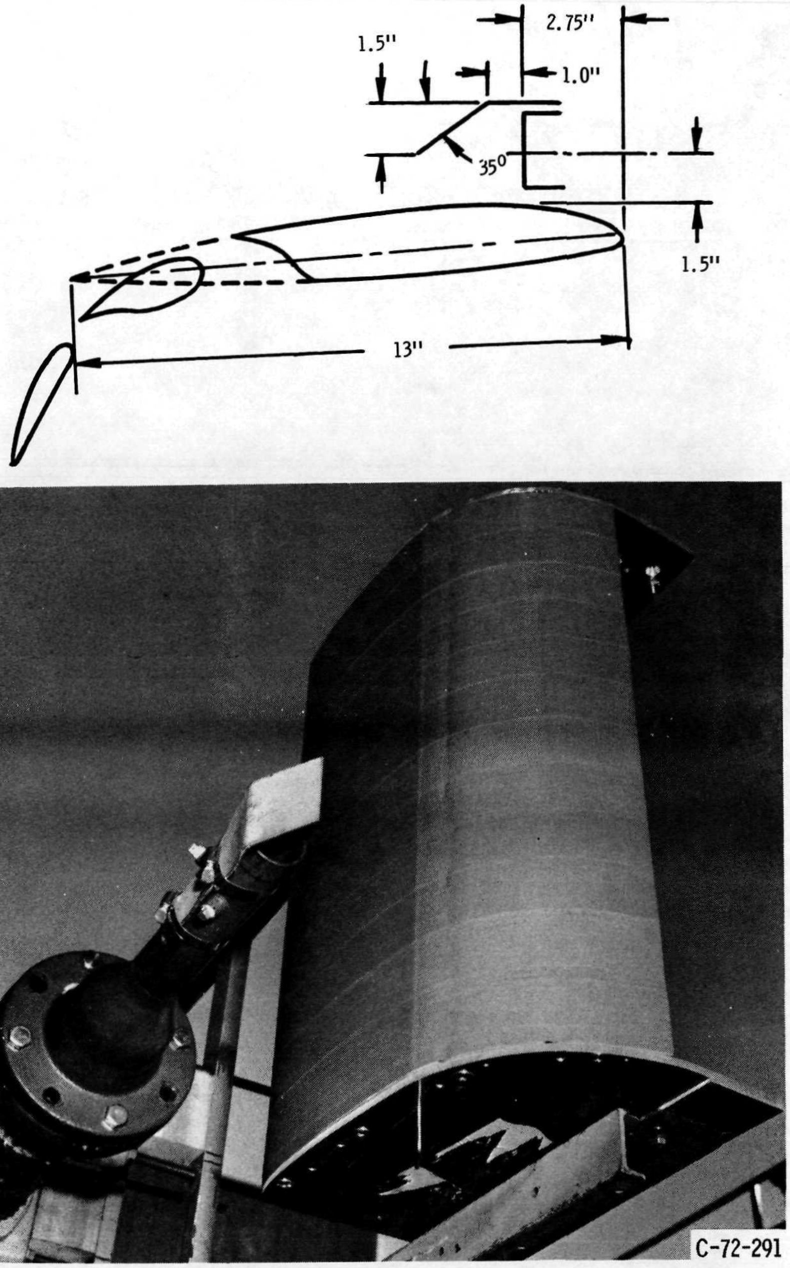

(a) CIRCULAR NOZZLE WITH COVERED SLOTS AND DEFLECTOR; 30°-60° FLAP SETTING.

Figure 6. - Typical test configurations of the engine-over-the-wing model.

E-7227

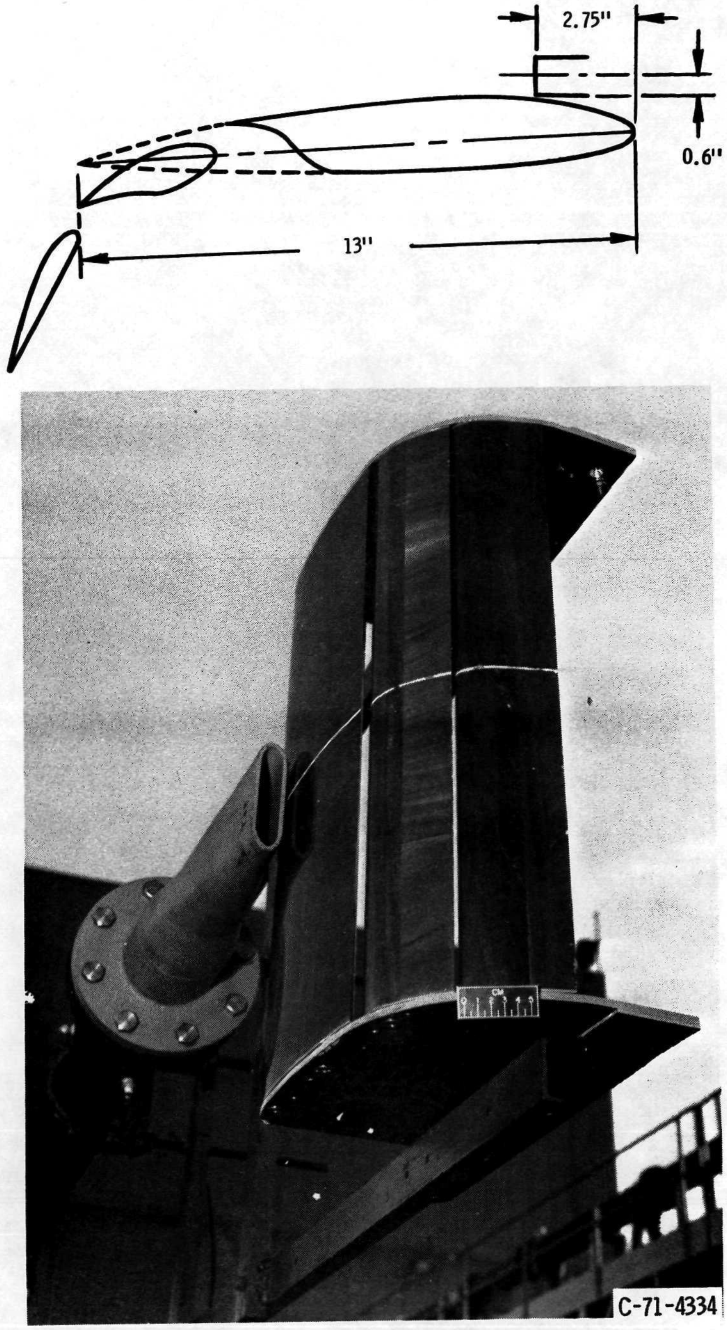

(b) SLOT NOZZLE; 30°-60° FLAP SETTING.

Figure 6. - Continued.

E-7227

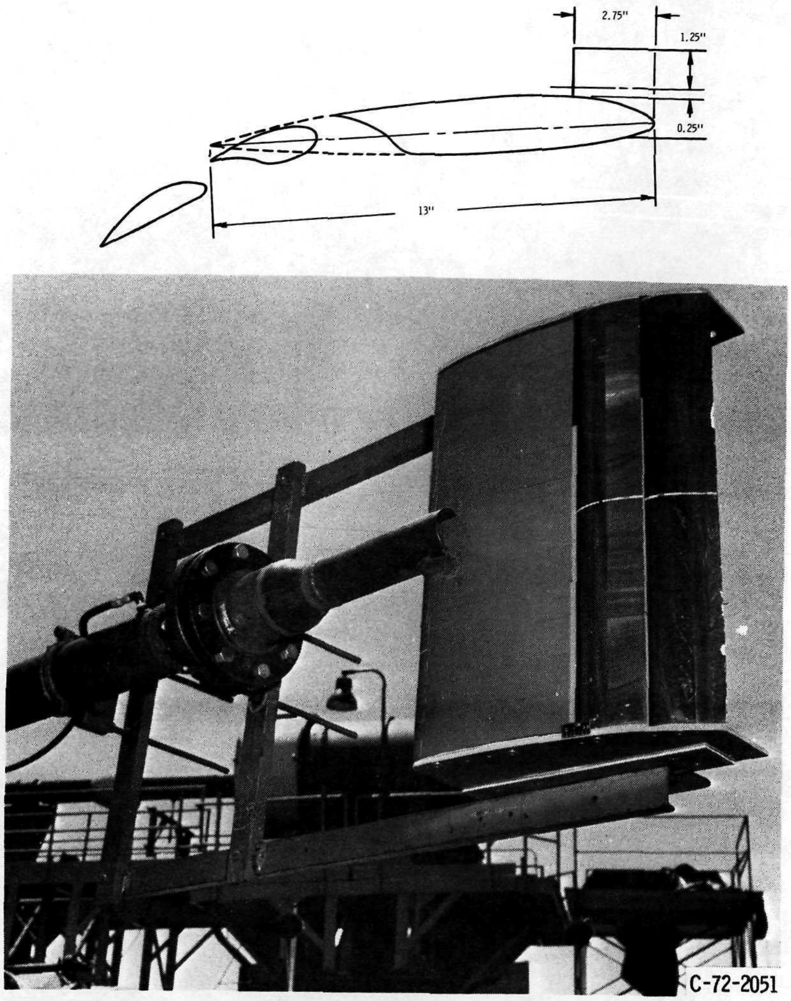

(c) D-SHAPED NOZZLE; 10^{0}-20^{0} FLAP SETTING.

Figure 6. - Continued.

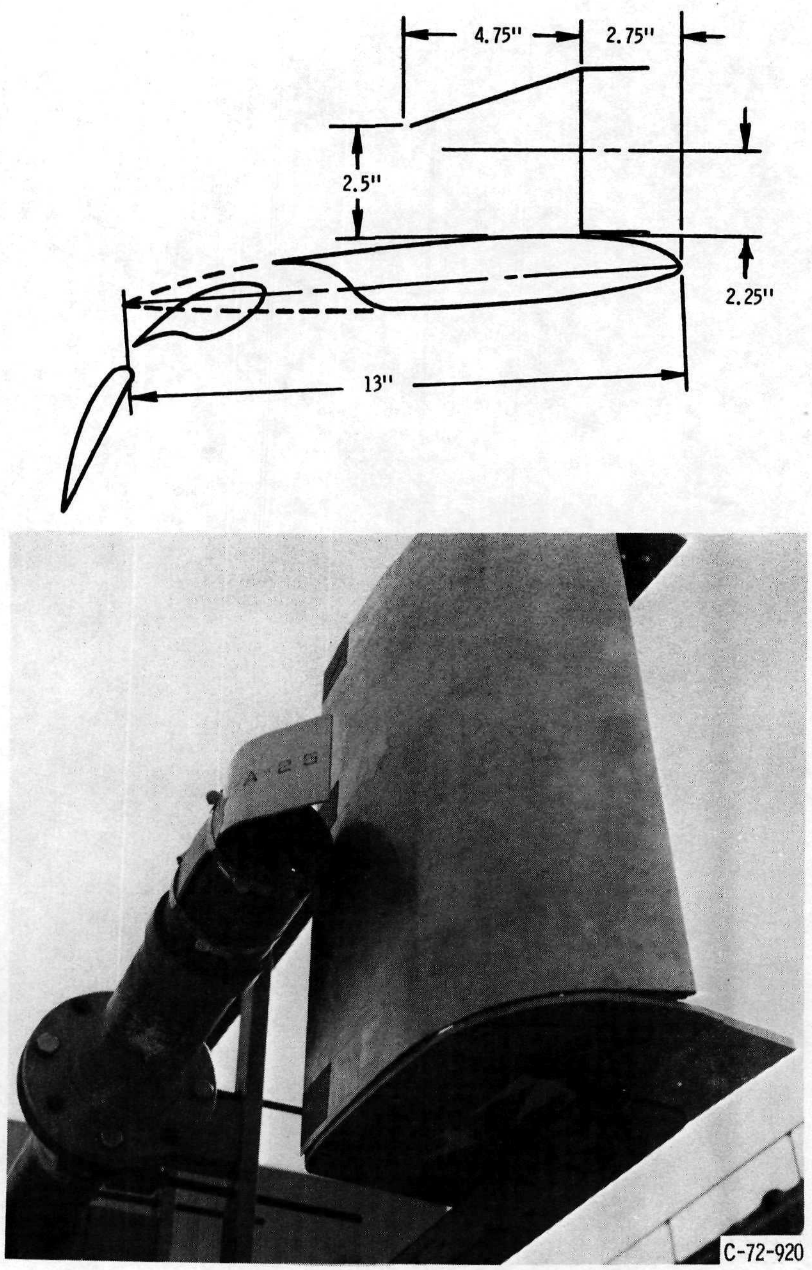

(d) MIXER NOZZLE WITH COVERED SLOTS AND DEFLECTOR; 30^{0}-60^{0} FLAP SETTING.

Figure 6. - Concluded.

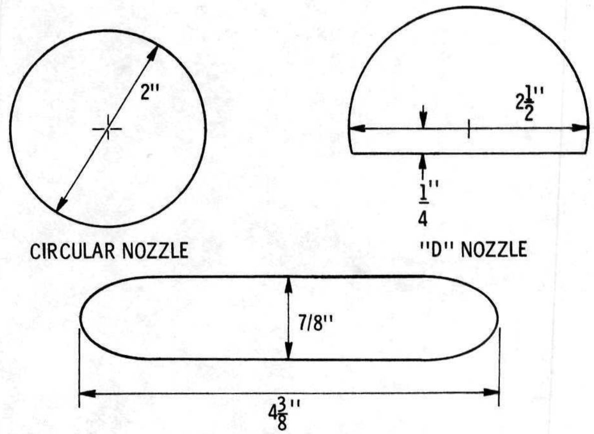

(a) NOMINAL 2'' EQUIVALENT DIAMETER NOZZLES.

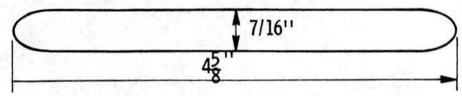

(b) 10:1 ASPECT RATIO SLOT NOZZLE (Ae = 2.09 IN.^{2})

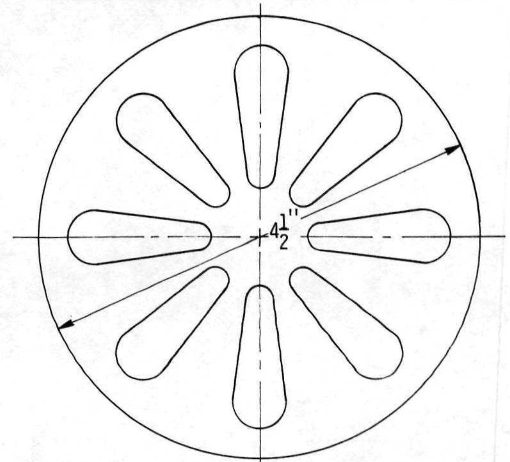

(c) 8-LOBE MIXER ORIFICE PLATE (De = 2.4 IN.)

Figure 7. - Nozzles used on the engine-over-the-wing model.

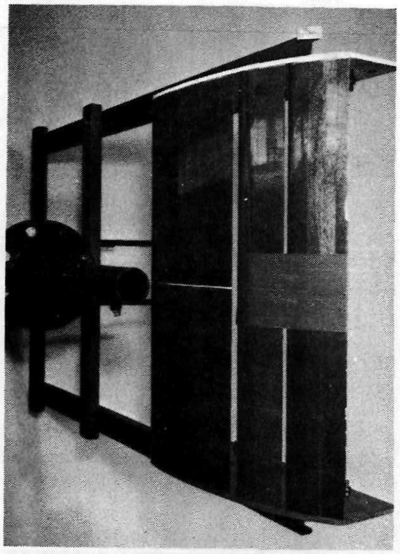

(a) SECOND SLOT COVERED WITH A 4 INCH WIDTH OF TAPE.

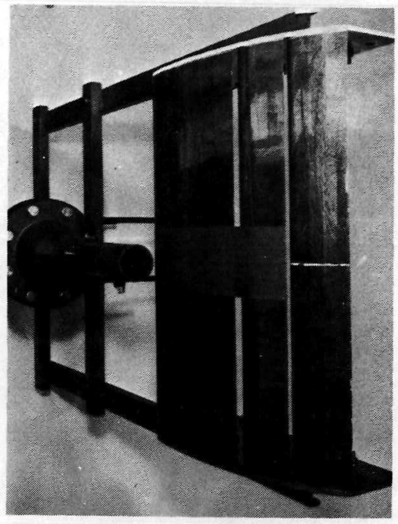

(b) FIRST SLOT COVERED WITH A 4 INCH WIDTH OF TAPE.

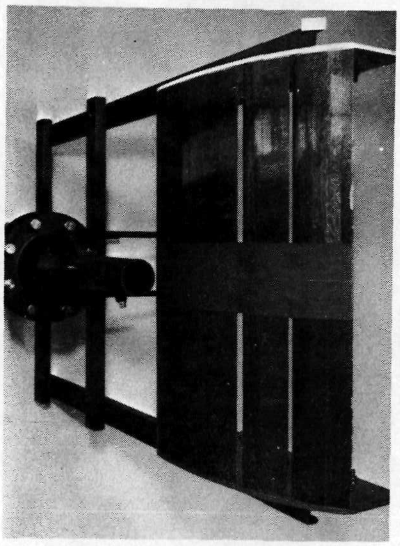

(c) BOTH SLOTS COVERED WITH A 4 INCH WIDTH OF TAPE.

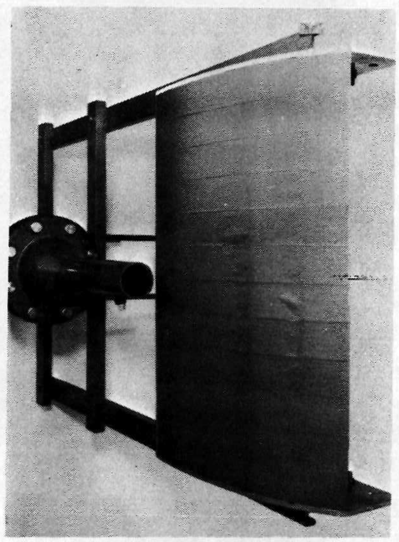

(d) FULLY COVERED SLOTS.

Figure 8. - The engine-over-the-wing model with various degrees of slot covering.

E-7227

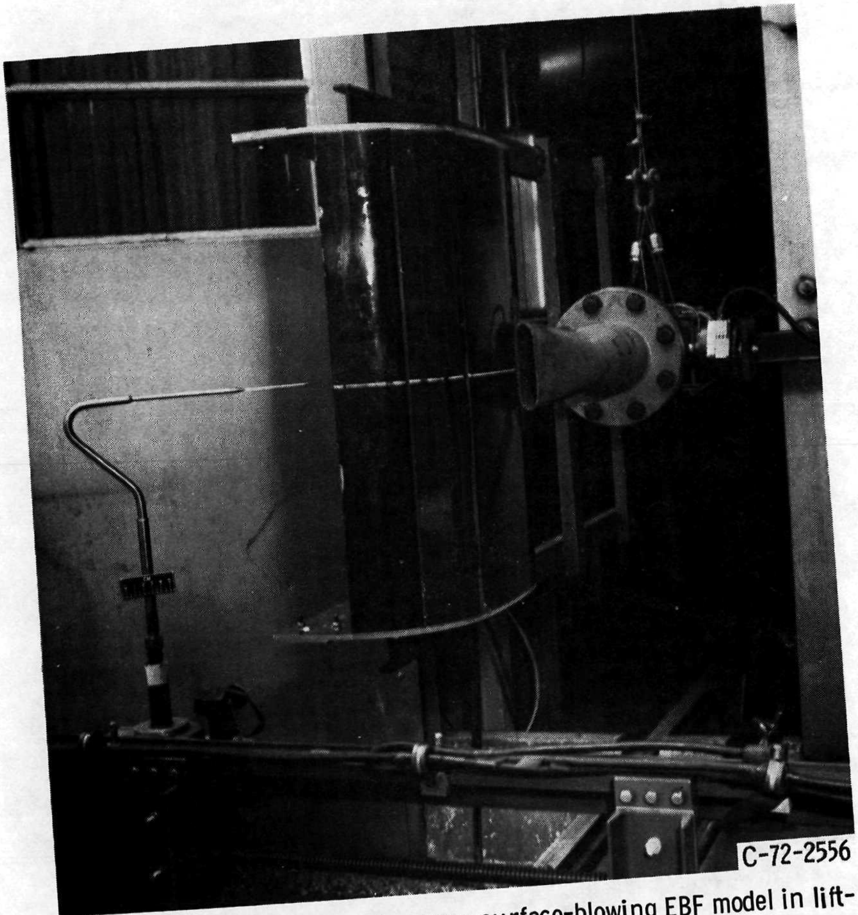

Figure 9. - A 5 to 1 slot nozzle upper-surface-blowing EBF model in lift-thrust rig.

E-7227

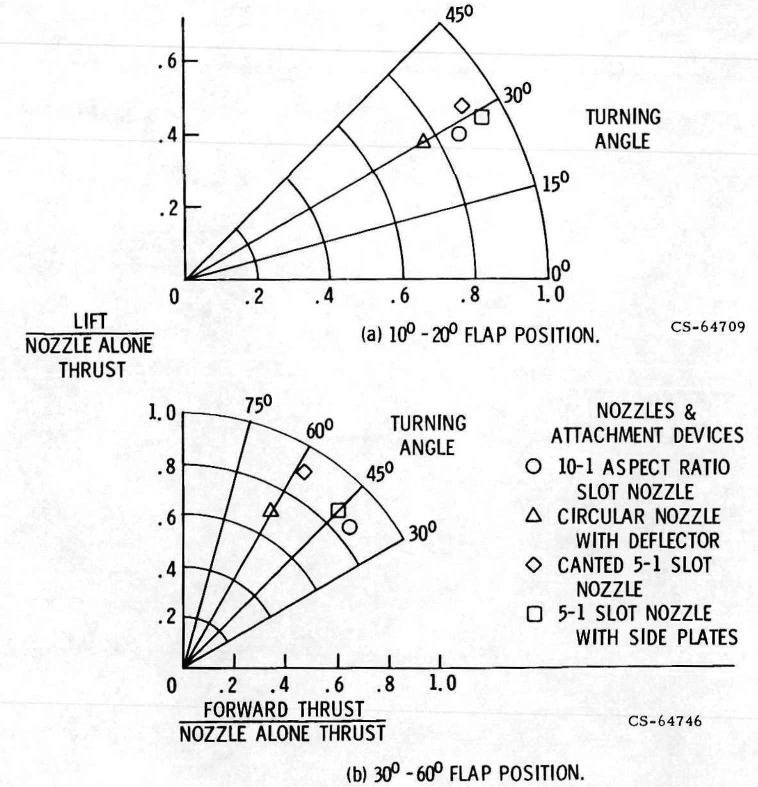

Figure 10. - Static turning effectiveness for some good attachment cases. Flap slots were covered.

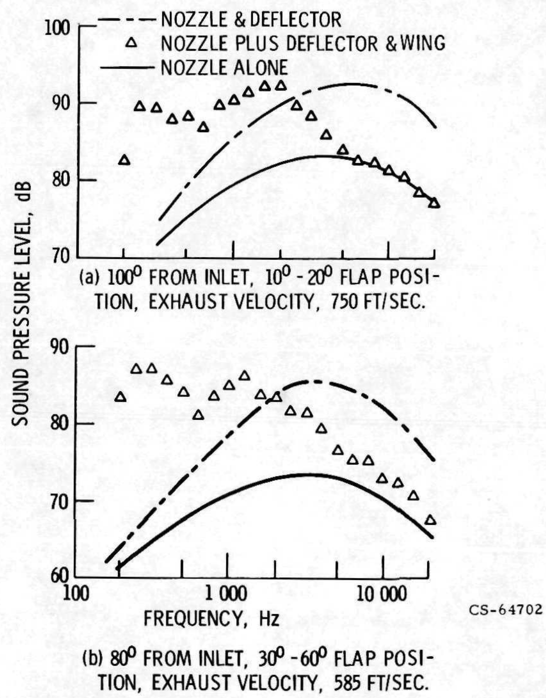

Figure 11. - Noise spectra with deflector configuration. Microphone distance, 10 ft. Circular nozzle diameter, 2 inches.

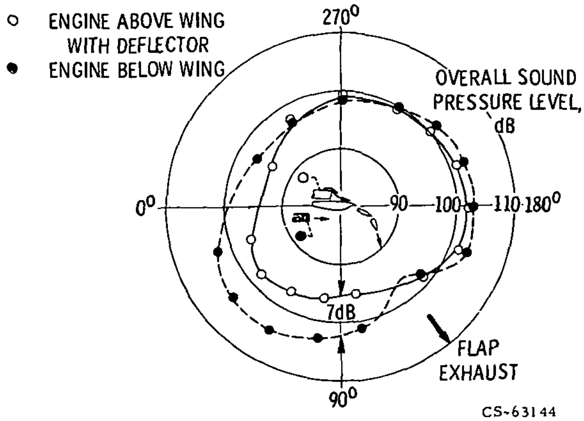

Figure 12. - Comparison of noise radiation patterns for externally blown flaps. Circular nozzle diameter, 2 inches. Flap angles, 30° - 60°. Exhaust velocity 585 ft/sec. Microphone radius, 10 ft.

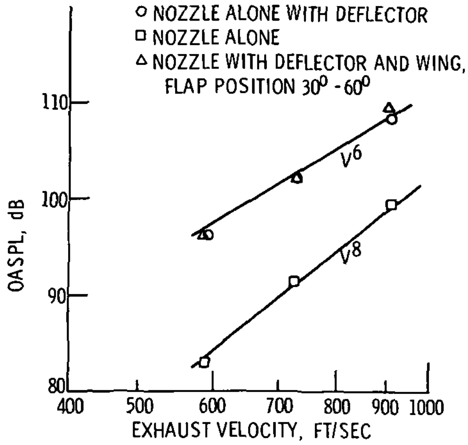

Figure 13. - Effect of exhaust velocity on OASPL for the circular-nozzle-with-deflector engine-over-the-wing model. Microphone angle, 80°

E-7227

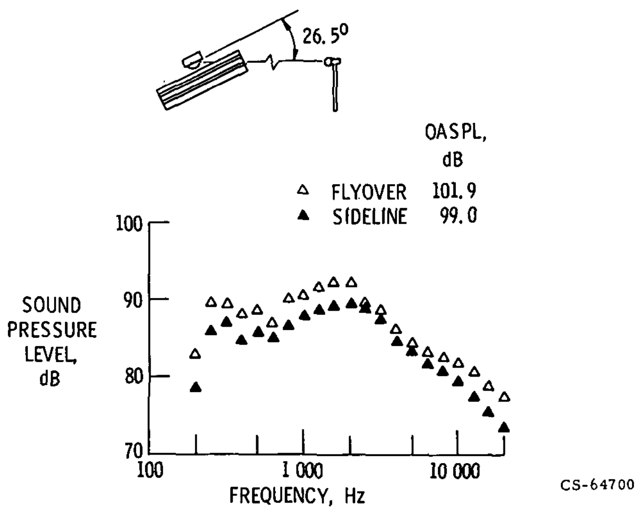

Figure 14. - Comparison of flyover and sideline 1/3-octave spectra for circular nozzle with deflector configuration. Flap position, $10^\circ - 20^\circ$. Microphone angle, 100°. Exhaust velocity, 750 ft/sec. Distance, 10 feet.

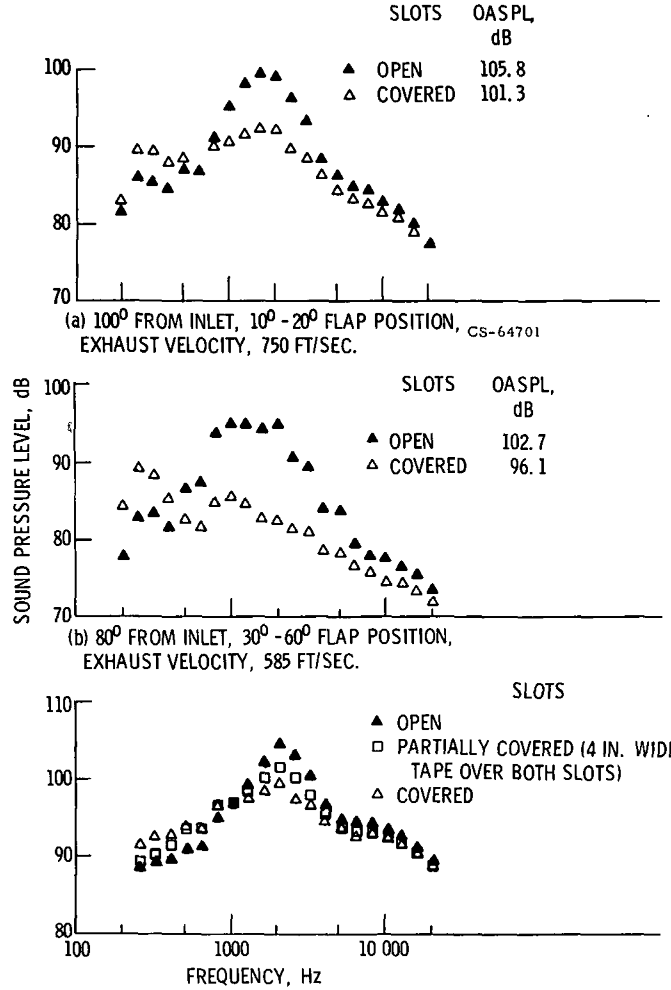

(c) MICROPHONE ANGLE, 100°. FLAP POSITION, $10^\circ - 20^\circ$. EXHAUST VELOCITY, 920 FT/SEC.

Figure 15. - Effect of covering flap slots on noise spectra. Circular nozzle with deflector configuration.

E-7227

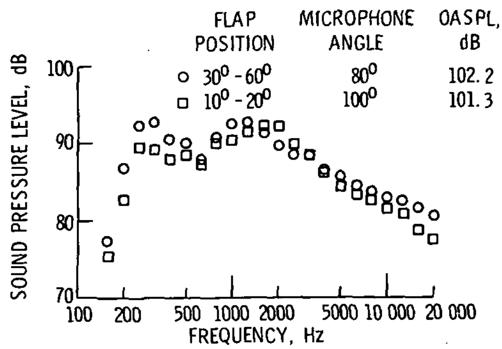

Figure 16. - Effect of flap position on noise spectra. Circular nozzle with deflector configuration. Exhaust velocity, 750 ft/sec.

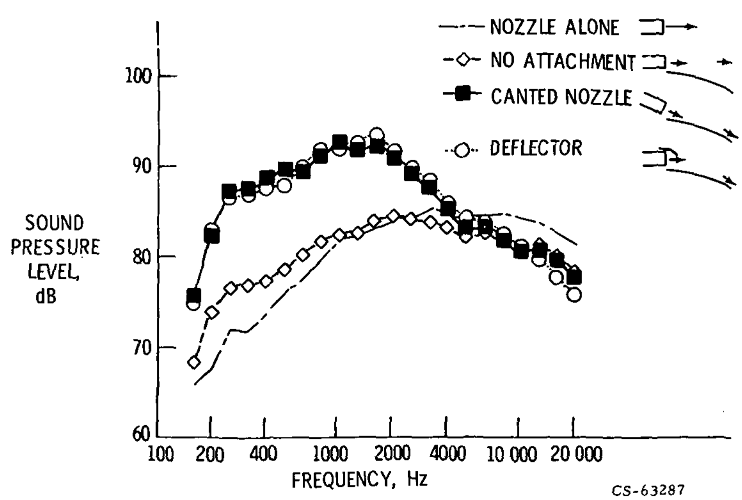

CS-63287

Figure 17. - Comparison of noise spectra for circular nozzle configurations. Microphone angle, 120^0. Distance, 10 ft. Flap position, $10^0 - 20^0$. Exhaust velocity, 750 ft/sec.

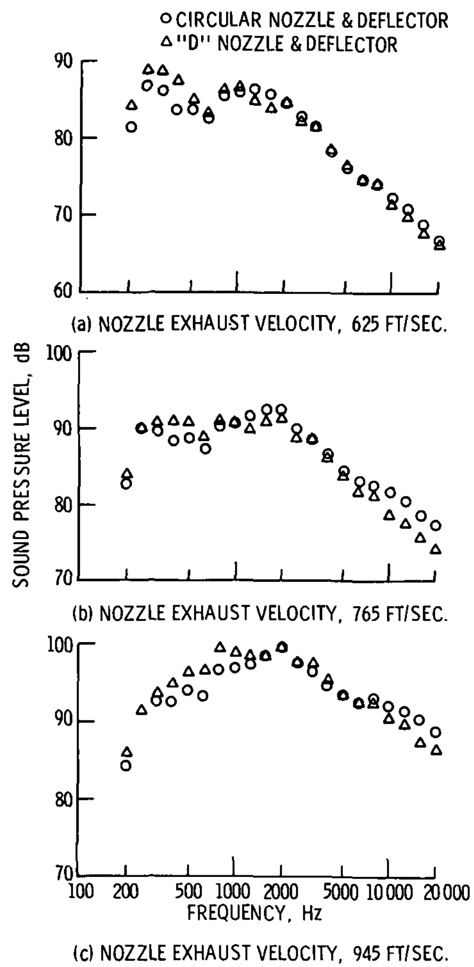

Figure 18. - Comparison of 1/3-octave spectra for circular nozzle and "D" nozzle configurations. Deflector attached. Microphone angle, 100°. Flap position, 10° - 20°.

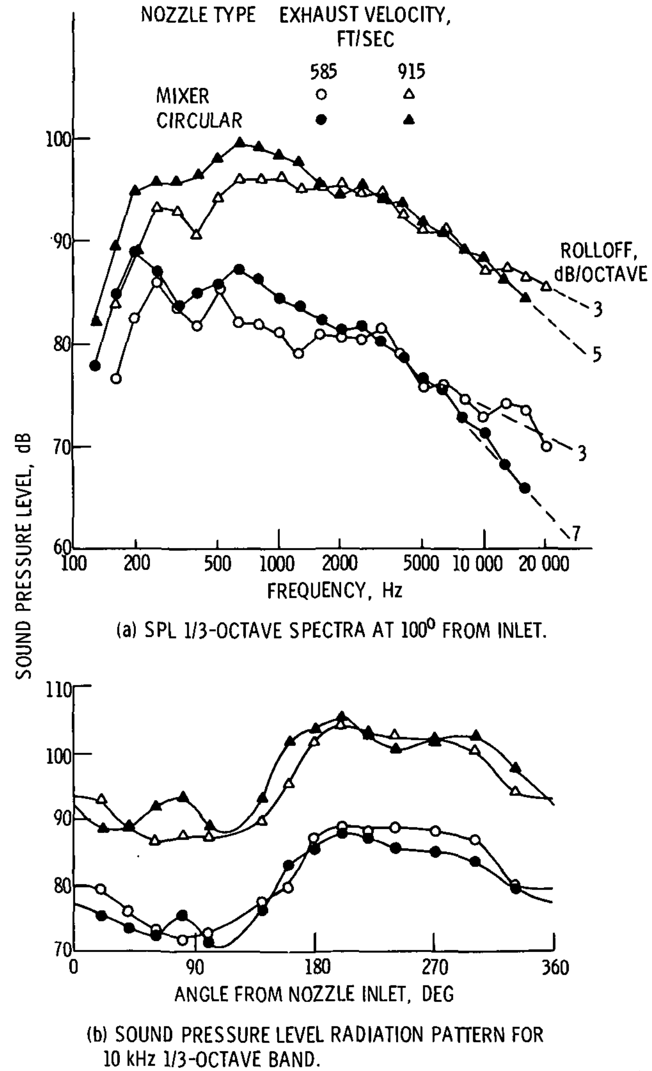

Figure 19. - Comparison of noise from mixer nozzle with deflector configuration with that from circular nozzle with deflector configuration. Flap angle, 30° - 60°. Circular nozzle data scaled to 2.4 in. diameter.

E-7227

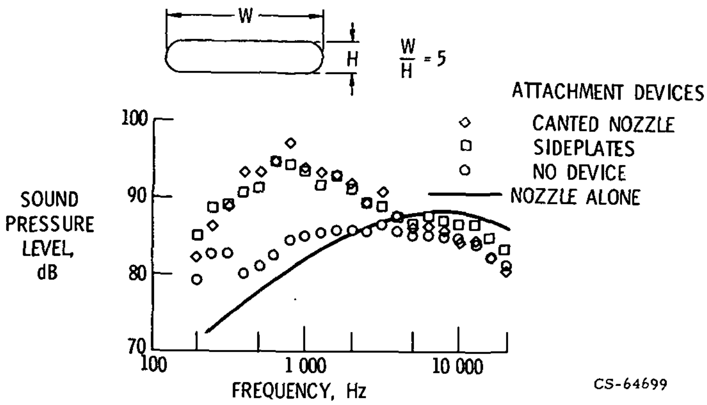

Figure 20. - Noise spectra for 5 to 1 slot nozzle configurations with various attachment devices. Slot area, 3.5 in.^{2}. Flap position, 10° - 20°. Microphone angle, 120°. Distance, 10 ft. Nozzle exhaust velocity, 750 ft/sec.

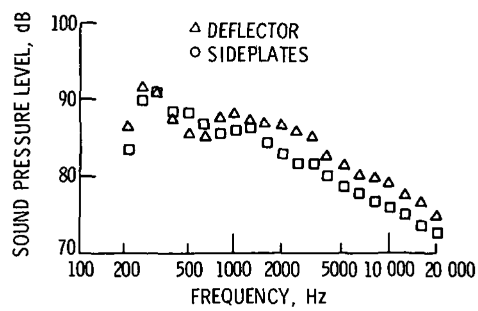

Figure 21. - Comparison of spectrum for 5 to 1 slot nozzle with deflector configuration with that for the 5 to 1 slot nozzle with sideplates. Microphone angle, 80°. Flap position, 30° - 60°. Nozzle exhaust velocity, 585 ft/sec.

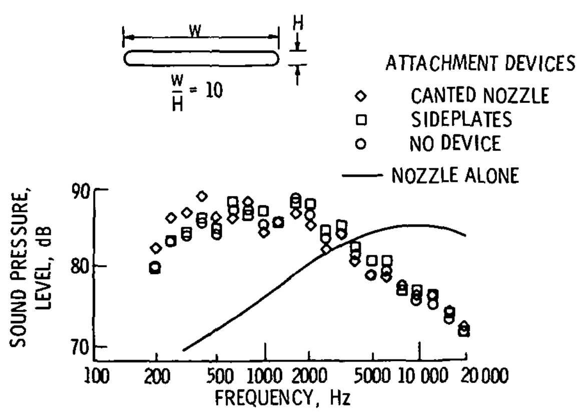

Figure 22. - Noise spectra for 10 to 1 slot nozzle configurations with various attachment devices. Slot area, 2.1 in.^{2}. Microphone angle, 120°. Distance, 10 ft. Flap position, 10° - 20°. Nozzle exhaust velocity, 750 ft/sec.

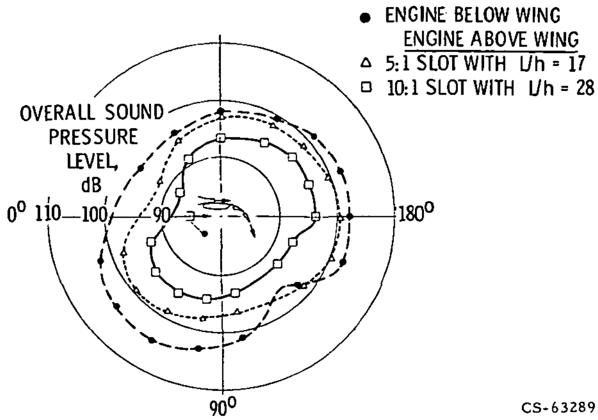

Figure 23. - Comparison of noise radiation patterns at 10 feet for externally blown flap models. Nozzle area, 3.5 in.^{2}. Flap position, 30° - 60°. Exhaust velocity, 585 ft/sec.

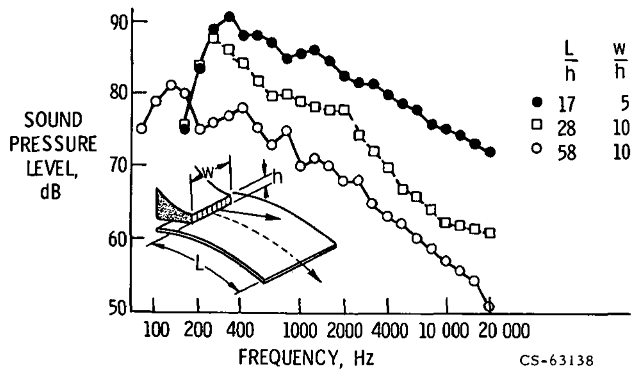

Figure 24. - Effect of wing-flap length to slot height ratio on noise for slot nozzle configurations. Microphone angle, 80°. Distance, 10 ft. Slot area, 3.5 in.^{2}. Flap position, 30° - 60°. Exhaust velocity, 585 ft/sec.

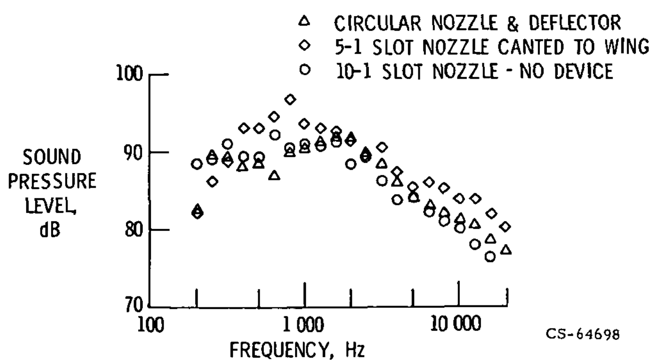

Figure 25. - Noise summary for some good attachment cases. Nozzle area, 3.5 in.^{2}. Microphone angle, 120°. Distance, 10 ft. Flap position, 10° - 20°. Exhaust velocity, 750 ft/sec.

E-7227

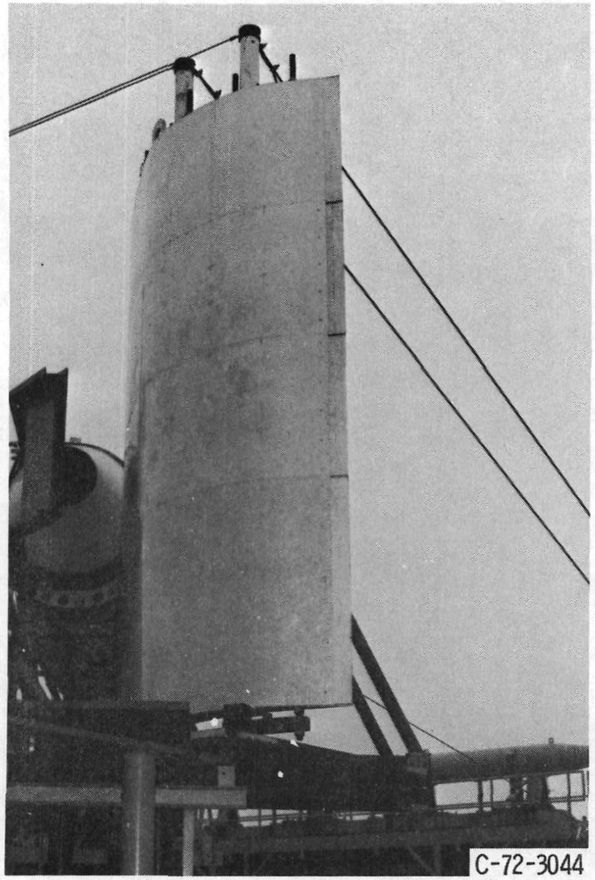

Figure 26. - Large scale engine over the wing externally blown flap model. Circular nozzle with deflector configuration. Nozzle diameter, 13 inch. Wing chord length, 7 feet.

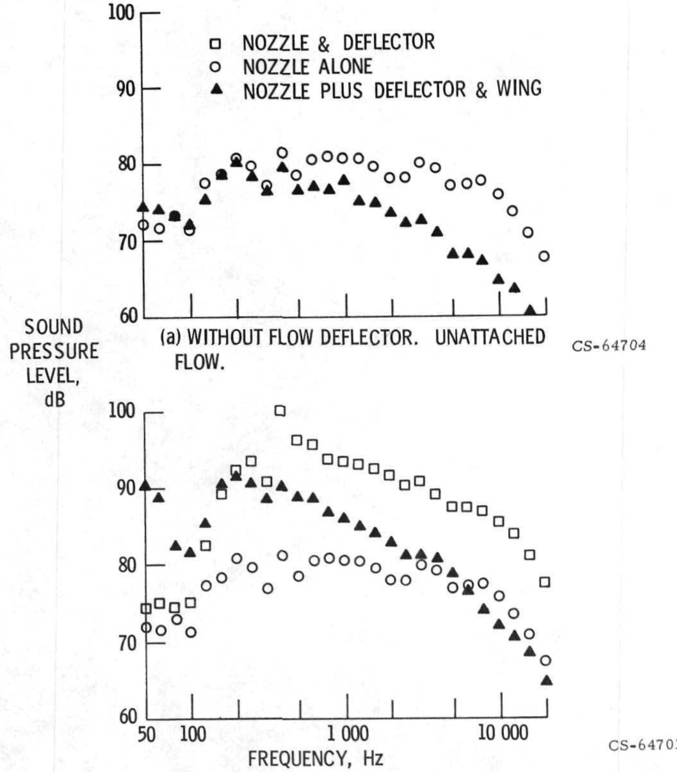

(a) WITHOUT FLOW DEFLECTOR. UNATTACHED FLOW.

(b) WITH FLOW DEFLECTOR. ATTACHED FLOW.

Figure 27. - Noise spectra at 90^0 from inlet for large-scale circular-nozzle engine-over-the-wing configuration. Distance, 50 feet. Nozzle diameter, 13 in. Flap position, 30^0 - 60^0. Slots covered. Exhaust velocity, 680 ft/sec.

E-7227

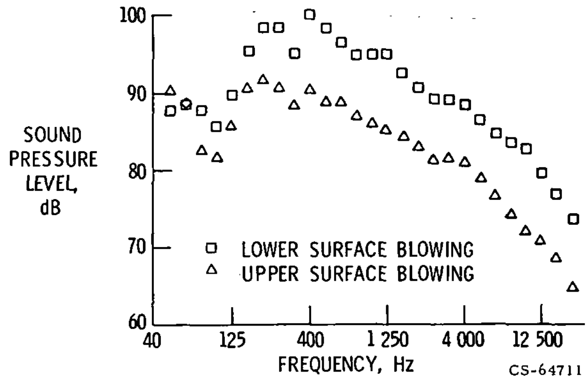

Figure 28. - Comparison of externally blown flap noise spectra. Microphone angle, 90°. Distance, 50 ft. Nozzle diameter, 13 inches. Flap position, 30° -60°. Exhaust velocity, 680 ft/sec.

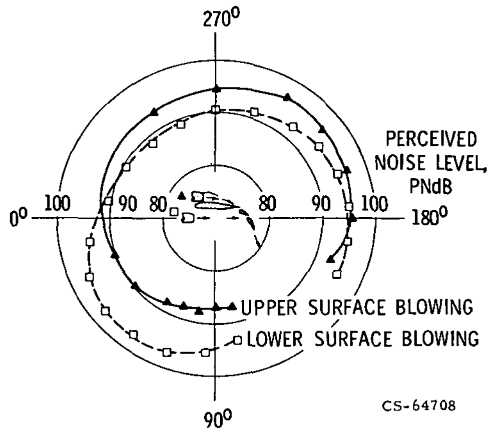

Figure 29. - Comparison of EBF perceived noise level patterns at 500 feet. Nozzle diameter, 13 in. Wing chord length, 7 feet. Flap position, 30° -60°. Exhaust velocity, 680 ft/sec.

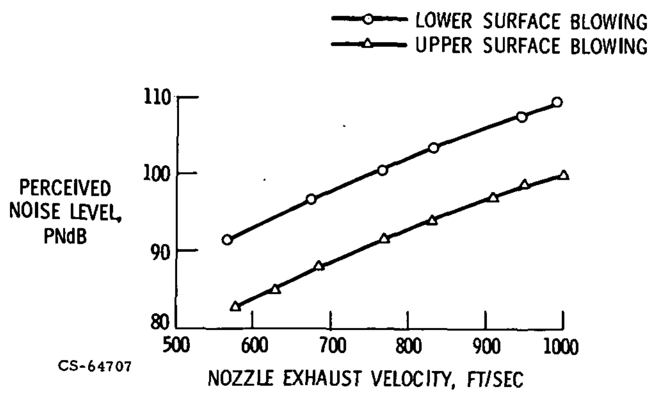

Figure 30. - Effect of nozzle exhaust velocity on EBF perceived noise level at 500 feet. Nozzle diameter, 13 in. Wing chord length, 7 feet. Flap position, 30° -60°.

E-7227

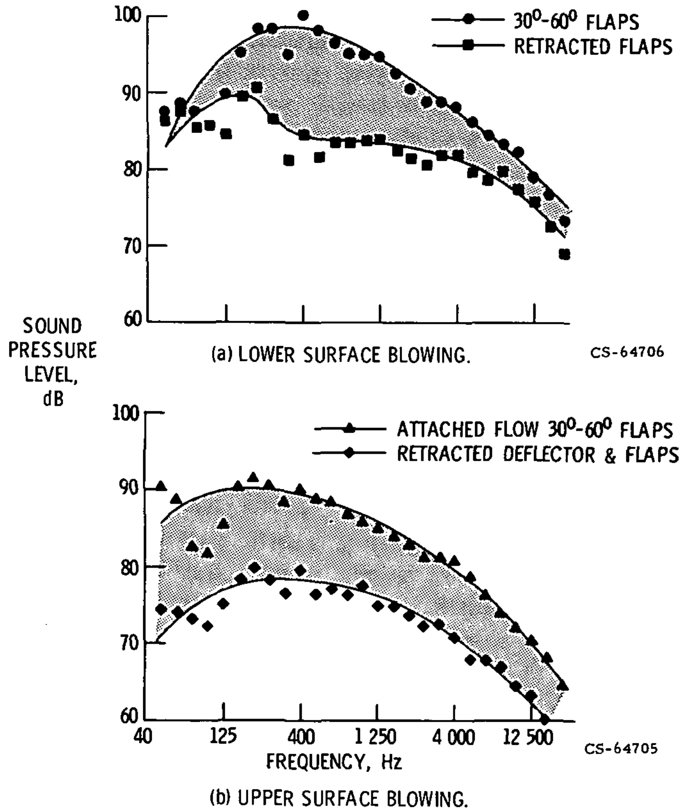

Figure 31. - Flap noise associated with flow turning. Nozzle diameter, 13 in. Wing chord, 7 feet. Microphone angle, 90°. Distance, 50 feet. Exhaust velocity, 680 ft/sec.

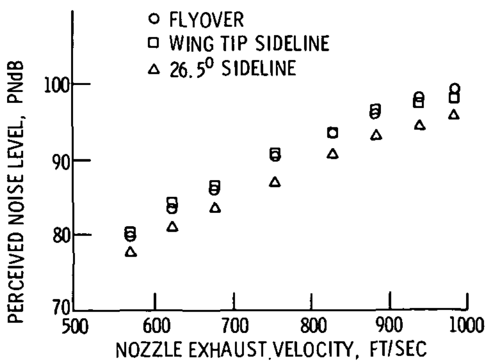

Figure 32. - Comparison of large model flyover and sideline perceived noise levels at 500 feet. Flap position, 10° - 20°. Microphone angle, 100°.

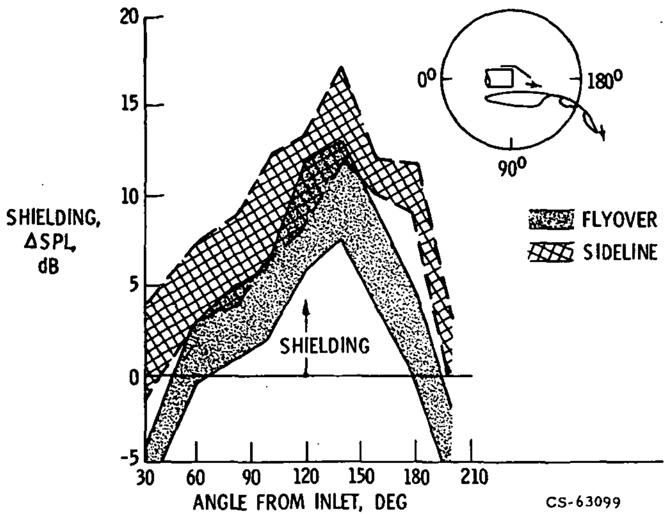

Figure 33. - Shielding effect on internal exhaust noise by slotless wing. Circular nozzle with deflector configuration. Wing chord length, 13 in. Flap position 30° - 60°. Exhaust velocity, 585 ft/sec.

E-7227